DC Restoration by Data-Aided Sequence in Kramers-Kronig Receiver

Zhonghan Su, Jiasi Yang, Jingcan Ma , Hanxiao Xue, Zhennan Zheng , Xinlu Gao , and Shanguo Huang

Abstract—In recent years, Kramers-Kronig (KK) receiver has been widely studied because of its simple structure and the ability of digital signal processing (DSP) to recover complex value signals. One practical structure is detecting the optical signal with an AC-coupled photodetector. However, the direct current (DC) component of the photocurrent will be lost, in which case the KK algorithm ceases to be effective. To restore the lost DC component, we propose a simple data-aided method to estimate the DC component by the information of signal mean power stored in the designed data-aided sequences. We introduce a correction coefficient to evaluate the accuracy of our DC estimation by comparing it to the conventional DC sweeping method. Furthermore, the coefficient can be used to combat the DC estimation deviation. We carry out both simulations and experiments to study the performance of the proposed method. The results show that the DC component can be effectively recovered and the system performance is close to the results of the DC sweeping method. At the same time, in the case of low optical signal-to-noise ratio, optimization of correction coefficient can effectively improve the system performance.

Index Terms—Kramers-Kronig receiver, digital signal processing.

I. INTRODUCTION

WITH the rapid growth of Big Data and Cloud Computing, researchers are focusing more on the communication between data centers [1]. Generally, the distances between two data centers are within 100km, and the cost-effective direct-detection (DD) method is preferred. Besides, the growing demand for transmission capacity and the limited bandwidth require higher-order modulation formats, such as quadrature amplitude modulation (QAM). However, QAM single sideband (SSB) signals will suffer from signal-signal beat interference (SSBI) after DD, because it has multiple amplitudes and the SSBI is no longer a constant but varies as the signal amplitude changes. We only consider SSB signals here because double side-band (DSB) signals after fiber transmission will have a frequency-dependent loss in the DD receivers. Traditionally the SSBI is mitigated by transmitting the SSB signal with a large carrier-to-signal power ratio (CSPR) or introducing a large protecting interval, which is two times the signal bandwidth at least. A large CSPR will increase the fiber nonlinear effect with the same signal power, or reduce the signal quality with the same overall power, while a large protecting interval will significantly reduce the spectrum efficiency. KK receivers have attracted much attention because of their ability to recover the complex-valued signal by using a single photodetector (PD) and eliminating SSBI without a large CSPR at the same time [2], [3]. Compared to the conventional coherent receiver, KK receivers do not need balanced PDs, thus the cost is much lower. Studies on the KK receivers have solved some practical problems [4]–[9]. KK receiver shows its advantages and competitiveness, especially in short-haul communications [10]–[15]. KK receiver needs the signal to meet the requirement of the minimum phase (MP) condition, and the optical signal is generally transmitted with the carrier with enough power. After square-law detection at the PD, there will be a large DC component in the electrical signal, resulting in a lower ratio of the payload signal and may introduce unwanted bias offset to the subsequent circuits. An AC-coupled PD is preferred to eliminate the DC component in such a situation [6]. For example, with AC-coupled PD, the output photocurrent without DC component can fully utilize the linear region of a regular electrical amplifier. However, the DC component is indispensable in the signal recovery algorithm in KK receivers [4]. How to restore the lost DC component becomes a problem.

There are several methods to estimate the DC component after the AC-coupled PD [3]–[6]. One simple way is to try all the possible values of the DC component and make judgments based on the bit-error ratio (BER) or error-vector magnitude (EVM) [3], which can achieve a wonderful BER performance but may cost much time. Another method is proposed in [4]. In this method, the CSPR of the signal is known before transmission, and the DC component is guessed based on this information. After signal recovery, the DC component is adjusted according to the system performance. A zero-light-padding method for SSB signal with a virtual carrier is proposed in [5]. It estimates the DC component directly from the zero preambles, which is effective and simple to apply. A simple one-step method is proposed in [6], the DC component is estimated by measuring and utilizing the statistical information of the electrical signal after square detection with the help of zero-padded preambles inserted at the beginning of the signal frame.

In this letter, we propose a simple data-aided method to estimate the DC component with data-aided sequences. The

data-aided method has been widely used in equalizations and synchronizations [16], [17]. Typically, these data-aided equalization or synchronization methods require a long training sequence to estimate the channel response and compensate for channel penalties. In these methods, the detailed phase information of the sequence is fully used. Our proposed data-aided method utilizes the information of the signal power without recovering the detailed information of the sequence. By designing data-aided sequences, the information of signal mean power and the carrier amplitude can be stored and can be recovered by simple calculations. Data-aided method does not require the receiver to know any prior information about the CSPR of the transmitted signal. The receiver only needs the information of the length of the designed sequence. Furthermore, it is unnecessary to repeat calculating BER or EVM by iteratively updating the estimation based on the BER or EVM performance. Our method has simple and flexible principles. We carry out both simulations and experiments to show its effectiveness. Compared to the traditional sweeping method, our method has similar performance but the time required is greatly reduced.

II. PRINCIPLES

Kramers-Kronig receiver requires the SSB signal to be transmitted with a carrier, which should be large enough to meet the MP condition that KK algorithm requires. Ignoring the noise issues, the optical SSB signal can be expressed as

$$E(t) = C + S(t) = C + A(t)e^{j[\pi Bt + \varphi(t)]}, \qquad (1)$$

Where C represents the optical carrier, B, $A(t)$ and $\varphi(t)$ represent the bandwidth, amplitude and phase of the payload signal S(t). To meet the MP condition, C is supposed to be larger than $A(t)$. The photocurrent generated by the AC-coupled PD with DC component suppressed can be expressed as

$$I(t) = |E(t)|^2 - P_{DC}$$
$$= C^2 + 2CA(t)\cos[\pi Bt + \varphi(t)] + A(t)^2 - P_{DC}, \quad (2)$$

$$P_{DC} = P_C + \overline{A(t)^2}. \qquad (3)$$

Here P_{DC} denotes the suppressed DC component, P_C denotes C^2 and $\overline{A(t)^2}$ denotes the average of $A(t)^2$. We rewrite $\overline{A(t)^2}$ as $\overline{P_S}$. In a typical KK receiver with DC-coupled PD, the detected SSB signal can be recovered by

$$\theta(t) = \frac{1}{2\pi}p.v. \int_{-\infty}^{\infty} \frac{\log[I(t') + P_{DC}]}{t - t'}dt', \qquad (4)$$

$$r(t) = \left\{\sqrt{I(t) + P_{DC}}e^{i\theta(t)} - C\right\}e^{-i\pi Bt}. \qquad (5)$$

It can be seen that the DC component is essential in KK receivers. However, with the AC-coupled PD, the P_{DC} is lost. To successfully recover the SSB signal, the P_{DC} has to be estimated and restored before utilizing the KK algorithm.

The value of the P_{DC} is actually a kind of power information, and we can put it on the power of the transmitted signal. In the proposed scheme we store the information of the P_{DC} in two data-aided sequences. The two sequences have different constant moduli. The first sequence has a modulus of $\frac{\sqrt{6}}{2}\sqrt{P_S}$,

and the second sequence has a modulus of $\frac{\sqrt{2}}{2}\sqrt{P_S}$. Thus, one data-aided sequence has a constant power of 1.5 times of $\overline{P_S}$ and another one has that of half of $\overline{P_S}$. It is reasonable to assume that the data-aided sequence does not influence the $\overline{P_S}$, because the total length of the sequence is generally short compared to the transmitted payload signal. After detected by AC-coupled PD, the generated photocurrent of two data-aided sequences can be expressed as

$$I_1(t) = \sqrt{6\overline{P_S}}C\cos[\pi Bt + \varphi(t)] + \frac{1}{2}\overline{P_S}, \qquad (6)$$

$$I_2(t) = \sqrt{2\overline{P_S}}C\cos[\pi Bt + \varphi(t)] - \frac{1}{2}\overline{P_S}. \qquad (7)$$

The phase in the cosine function is designed to be stochastic, which is generally satisfied when the sequence contains enough symbols, and the mean value of the cosine issues in photocurrent can be regarded as zero. The phases of the sequence symbols should be evenly distributed between 0 and 2π, to make sure the mean of the first item is 0.

By measuring the value of $I_1(t)$ and $I_2(t)$, we can estimate the value of $\overline{P_S}$ as

$$\overline{I_1(t)} = \overline{\sqrt{6\overline{P_S}}C\cos[\pi Bt + \varphi(t)] + \frac{1}{2}\overline{P_S}} = \frac{1}{2}\overline{P_S}, \qquad (8)$$

$$\overline{I_2(t)} = \overline{\sqrt{2\overline{P_S}}C\cos[\pi Bt + \varphi(t)] - \frac{1}{2}\overline{P_S}} = -\frac{1}{2}\overline{P_S}, \quad (9)$$

$$\widehat{\overline{P_S}} = \overline{I_1(t)} - \overline{I_2(t)}. \qquad (10)$$

Furthermore, the DC component P_C contributed by carrier C can be deduced from formula (6), by conducting the square of the first term on the right, as:

$$\left(I_1(t) - \frac{1}{2}\overline{P_S}\right)^2 = 3\overline{P_S}P_C(1 + \cos[2(\pi Bt + \varphi(t))]). \qquad (11)$$

Also, from formula (7), we have:

$$\left(I_2(t) + \frac{1}{2}\overline{P_S}\right)^2 = \overline{P_S}P_C(1 + \cos[2(\pi Bt + \varphi(t))]). \quad (12)$$

Therefore, P_C can be estimated by

$$\widehat{P_C} = \frac{\overline{\left(I_1(t) - \frac{1}{2}\overline{P_S}\right)^2} - \overline{\left(I_2(t) + \frac{1}{2}\overline{P_S}\right)^2}}{2\widehat{\overline{P_S}}}. \qquad (13)$$

With the estimation of $\overline{P_S}$ and $\overline{P_C}$, we can retrieve the received payload signal $r(t)$ by KK algorithm

$$\theta(t) = \frac{1}{2\pi}p.v. \int_{-\infty}^{\infty} \frac{\log\left[I(t') + \widehat{\overline{P_S}} + \widehat{P_C}\right]}{t - t'}dt', \qquad (14)$$

$$\widehat{r(t)} = \left\{\sqrt{I(t) + \widehat{\overline{P_S}} + \widehat{P_C}}e^{i\theta(t)} - \sqrt{\widehat{P_C}}\right\}e^{-i\pi Bt}. \quad (15)$$

Therefore, once we have received the data-aided sequence I_1 and I_2, we can use equation (10) to estimate $\overline{P_S}$, and then use equation (13) to estimate the $\overline{P_C}$.

The theoretical analyses above are under the assumption that there is no noise and no other system distortion. To evaluate

the accuracy of our proposed method in a practical system, we define a coefficient α.

$$\widehat{P} = \alpha \times \left(\widehat{P_C} + \widehat{P_S} \right). \tag{16}$$

Here $\hat{P}$ represents the estimated P_{DC} after correction. By sweeping the value of α, we essentially sweep the P_{DC}. So, we can find out the optimal power estimation to apply, the deviation between estimation and the optimal value, and how the deviation influences the system performance.

III. SIMULATIONS AND EXPERIMENTS

A. Simulations

We first carry out simulations to verify our principles. The symbol rate is 3 GBaud, which is the same as the subsequent experiments. In the simulation, the higher symbol rate only affects the performance of OSNR, and there is little difference in the accuracy of the proposed method. The pulse shaping here is root-raised cosine with a roll-off factor of 0.1. We also introduce a gap to avoid overlapping after the square-law detection at PD. The gap here is defined as the difference between the carrier frequency and the edge of the signal spectrum under an ideal roll-off factor equal to zero. The roll-off factor does not influence the accuracy of our proposed method, but the gap should be large enough for the bandwidth after pulse shaping. The data-aided sequence here consists of two const amplitude zero auto-correlation (CAZAC) sequences with different amplitudes as in principles. CAZAC sequences are generally used for synchronizations and equalizations [16], [17]. As we mentioned in the principles, the detailed information in the sequences is not essential to our estimation method, as long as the sequences satisfy the principle. Therefore, if a data-aided equalization method is used, our method can be easily applied by utilizing the existing CAZAC sequences. However, if data-aided equalization is adopted, it generally acquires a sufficiently long sequence to do channel estimation, which is much longer than the sequence that our method requires. The effects of different lengths of data-aided sequences on the efficiency of data-aided equalization [17] are investigated. The optical signal noise ratio (OSNR) here is 20 dB and the CSPR is 10 dB. Here the OSNR is defined as the ratio of the total power, which contains the carrier power and the payload signal power, to the noise power with the resolution of 0.1 nm. The equalization performance is evaluated by error vector magnitude (EVM), and the results are represented in Fig. 1. As Fig. 1 shows, the data-aided equalization method converges when the data-aided sequence has an adequate length. The length that our DC estimation method requires is much shorter compared to the length that equalization requires. After convergence, the data-aided equalization shows similar performance as blind equalizations, such as constant modulus algorithm (CMA), multi-modulus algorithm (MMA), and decision-driven least mean square (DDLMS) [18], [19] does. We utilize blind equalizations in later simulations and experiments.

We also compare our method to the existing zero-padding method [6]. We estimate the accuracy of the zero-padding
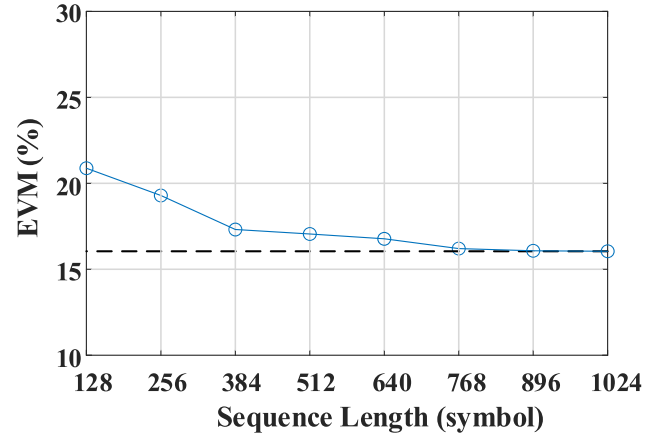

Fig. 1. Simulation results of data-aided equalization method with different lengths of data-aided sequences. The dashed line represents the EVM that the equalization converges.

method and the data-aided method, the estimation error is defined as

$$error = \frac{\widehat{P} - P_{DC}}{P_{DC}} \tag{17}$$

Here the P_{DC} is calculated before wiped out by the AC-coupled PD and $\hat{P}$ is the estimation. The OSNR here is 20 dB and the CSPR is 10 dB. The same blind equalization method is utilized in two estimation methods. We calculate the absolute values and the variances of estimation errors under the same symbol length that participates in the algorithm. The results are shown in Fig. 2. Compare to the zero-padding method, the data-aided method shows better performance on the mean value and the variance when the sequence is shorter, which verifies the accuracy and stability of our proposed method.

We also investigate the system performance with the proposed data-aided DC estimation method. The data-aided sequence consists of two kinds of CAZAC sequences with different amplitudes and its length is 1024, which is about 2% of the total length. Fig. 3 shows the simulation results 16 QAM signals with different CSPRs and OSNR with constant optical power and ideal PD. By varying the CSPR and OSNR, the percentage of payload signal power in overall power is adjusted. Since the BER becomes extremely small when OSNR is high, we evaluate the quality of the signal by EVM. By sweeping different values of α, we equivalently adopt the traditional DC sweeping method to find out the optimal value with which the system has the lowest EVM. We define the results with α equal to 1 as the results of the proposed data-aided method. The lowest EVM with optimal α as the sweeping results. Also, we record the EVMs with different α applied to find out the tendency.

In Fig. 3(a), the standard results of 16QAM signals are represented by the solid lines and the improved results are the dashed lines. The two lines are so close that there is nearly no difference when OSNR is low, and a little degradation within 1% can be obtained when OSNR is higher. Under a constant overall power, higher CSPR means lower payload signal power. When OSNR is low, a lower CSPR can improve the system performance because
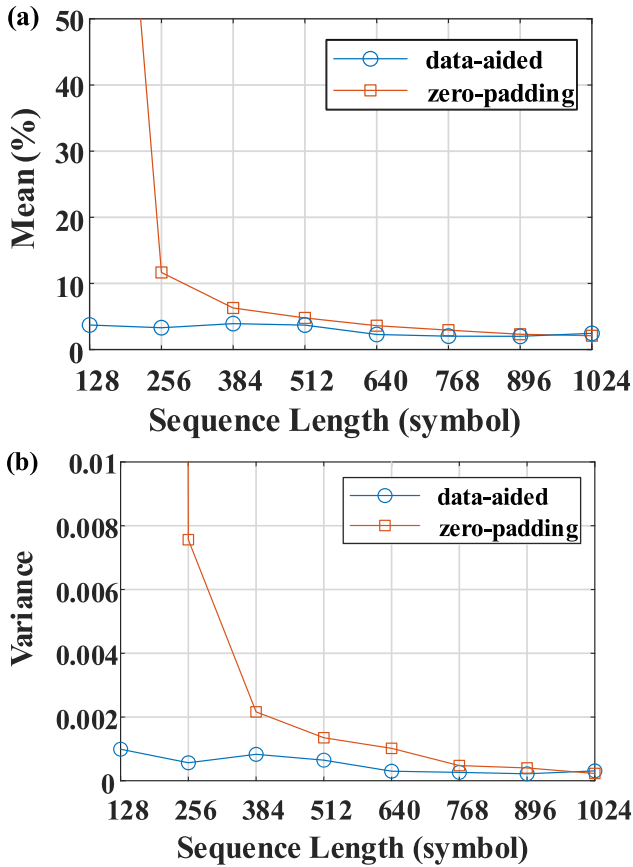
(a)

(b)

Fig. 2. Comparison of zero-padding method and data-aided method. (a) Mean of the absolute value of the estimation error. (b) the variance of the estimation error.
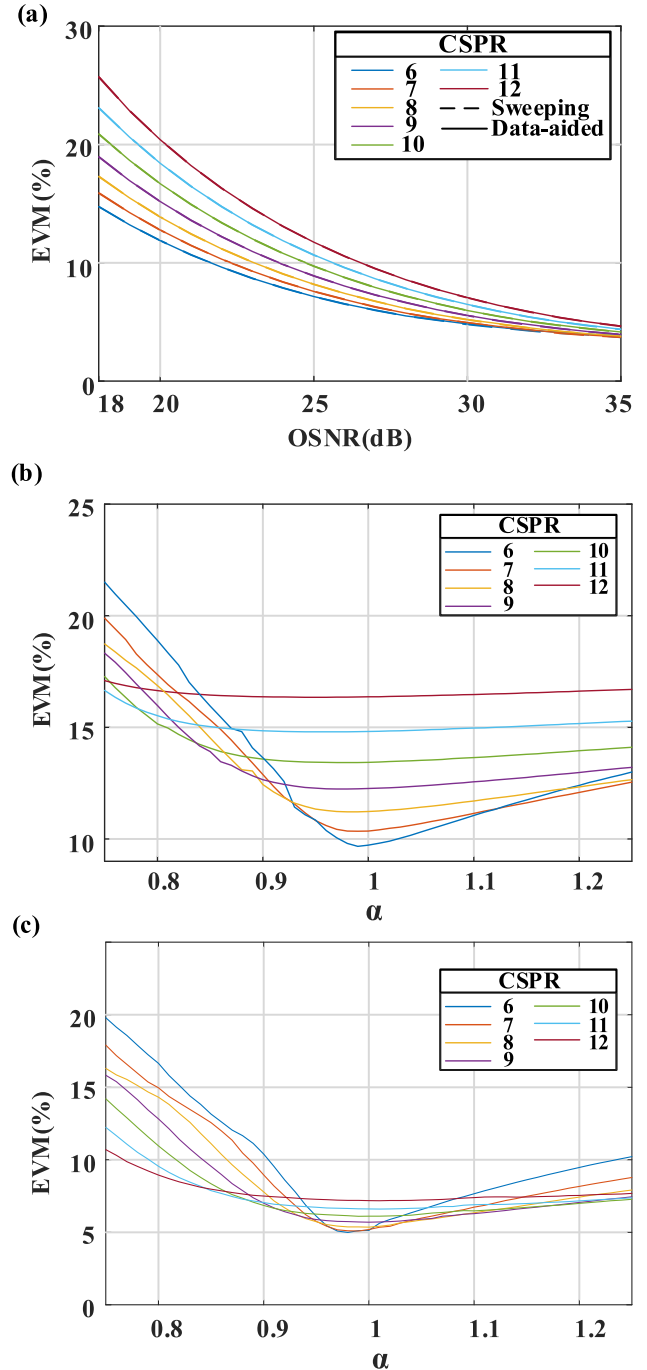
(a)

(b)

(c)

Fig. 3. Simulation results of 16QAM signals. (a) EVMs under various CSPRs and OSNRs. Solid lines are the results of proposed method and dashed lines are the results of the sweeping method. (b) EVMs with different α applied, where OSNR is 22 dB. (c) EVMs with different α applied, where OSNR is 30 dB.

it provides more signal power. While with a higher OSNR, such improvement is not evident, which is also shown in Fig. 3(b) and 3(c). The difference of EVM between CSPR equal to 6 and 12 is about 7% when OSNR is 22 dB, and about 3% when OSNR is 30 dB. Besides, the tendency of EVM over α under OSNR equal to 30 dB is similar to that under OSNR equal to 22 dB. The estimation performance varies more violently when CSPR is low and becomes flat as CSPR grows higher. In a practical system, a slightly higher CSPR is more preferred as it provides a larger redundant space for DC component fluctuations. The optimal α appears around 1 under two different OSNRs, and the deviation of α is less than 2%, indicating the accuracy of our method. Also, the EVM penalty from our estimation is negligible compared to the results of the traditional sweeping method, and it is unnecessary to sweep α for performance improvement.

B. Experiments

Transmission experiments have been conducted to evaluate the performance of our proposed method. The transmission experiment setup is illustrated in Fig. 4. A 3 GBaud 16-QAM data sequence is first generated, and the designed data-aided sequence is added before the payload data sequence. The length of the data-aided sequence is 1024 as we applied in simulations. An analog signal is generated by using an arbitrary waveform

generator (AWG) operating at 12 GSa/s and fed to an IQ modulator after introducing a 1.8 GHz offset by AWG. The roll-off factor here is 0.1 and there is a gap of 300 MHz due to the frequency offset as in simulations, which is 10% of the bandwidth. Both tunable CW lasers operate at 1550 nm with 100 kHz linewidth. One for the modulation, the other serves as the carrier. If only one laser is utilized to form the SSB signal, a typical method is to control the carrier power by adjusting
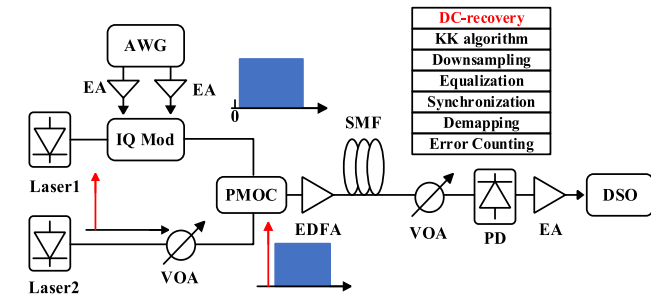
Fig. 4.　Experiment setup. In the back-to-back scenario, the EDFA and the fiber are not adopted. VOA: Variable optical attenuator. AWG: Arbitrary waveform generator. IQ Mod: IQ modulator. PMOC: Polarization-maintaining optical coupler. EDFA: Erbium-doped fiber amplifier. EA: Electrical amplifier. DSO: Digital storage oscilloscope.
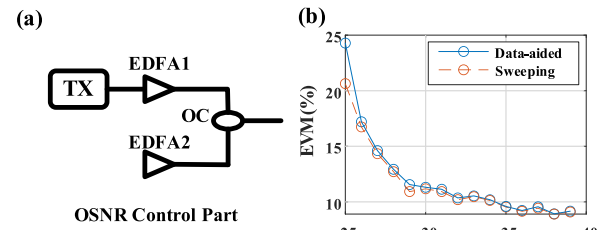

Fig. 5.　Experiments on OSNR. (a) Control setup. (b) EVMs under various OSNRs. CSPR here equals to 10 dB. Solid lines are the results of the proposed method and dashed lines are the results of the sweeping method.
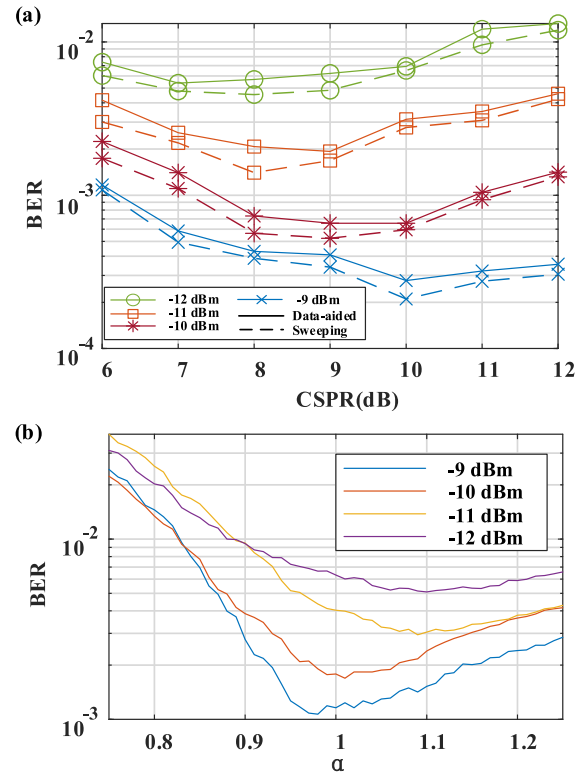

Fig. 6.　Back-to-back experiment results. (a) BERs under different received signal power and CSPRs. Solid lines are the results of the proposed method and dashed lines are the results of the sweeping method. (b) BERs with different α applied under different received power and CSPR equals 6 dB here.

the bias of the modulator. In such conditions, the signal cannot make full use of the linear area of the modulator. To cover the linear area as much as possible to improve the signal SNR after modulation, the signal is modulated at the carrier suppression point, and the carrier is provided by another laser. We use AWG to introduce the frequency gap instead of tuning the laser because AWG can provide a more accurate frequency offset. The two beams combine to form the desired optical SSB signal, whose CSPR can be adjusted by the variable optical attenuator (VOA) after laser2. The optical spectrum schematics before and after the polarization-maintaining optical coupler (PMOC) are also shown in Fig. 4. After the confluence, the SSB signal is transmitted and directly detected by an AC-coupled PD with a responsivity of 0.65 A/W in the back-to-back scenario. In a fiber transmission scenario, the optical signal is first amplified by an erbium-doped fiber amplifier (EDFA), then goes into the single-mode fiber (SMF) and is detected by the same AC-coupled PD. The electrical signal generated by PD is then amplified by an electrical amplifier (EA) and captured by a digital storage oscilloscope (DSO) working at 80 GSa/s. Then the digital signal generated is sent to the digital signal processor (DSP), whose diagram is also shown as an inset in Fig. 4. The digital signal is first resampled, and the beginning is found by correlation peaks utilizing CAZAC sequences. Then the DC component recovery method we proposed is adopted. The DC component restored is used for the later KK algorithm. After the KK algorithm, the recovered signal goes through blind equalizations mentioned before and a single-stage blind phase search (BPS) algorithm for carrier phase recovery. Then the frame synchronization is adopted. At last, the EVM and BER are evaluated.

We first investigate the system performance versus OSNR. The OSNR is controlled by introducing extra noise with the help of an EDFA without input laser as Fig. 5(a) shows. The OSNR is measured by a spectrometer. The CSPR is set to 10 dB and the optical power is enough. The definition of legends is the same as it in simulations.

As Fig. 5(b) shows, our method has similar performance compared to the simulation results, only with a penalty of several dBs. The solid line representing the EVM evaluated with our proposed method is very close to the dashed line representing the lowest EVM evaluated with the sweeping method. It shows

that even under a low OSNR, the deviation of the EVM is nearly negligible, and a larger penalty only appears when OSNR is very low.

We then investigate the BER performance of different CSPRs and received optical signal power in the back-to-back scenario. The CSPR is controlled by adjusting the VOA after the laser2, and the overall power is suppressed by another VOA before the AC-coupled PD to test the receiver sensitivity. The VOAs both work under the constant power method for a stable performance. Also, we find out the optimal α as in simulations by sweeping α and comparing BERs. Here we use BER instead of EVM to represent the system performance. The back-to-back results are given in Fig. 6. The definitions are the same as in simulations.

Fig. 6(a) shows the BER performance of the transmission system under different CSPRs and received optical signal power.
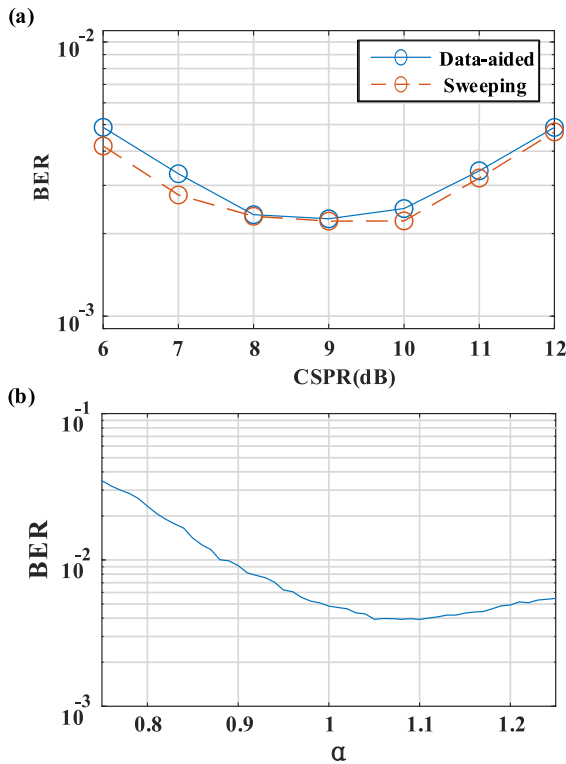
(a)

(b)

Fig. 7. Fiber transmission results. (a) BER performance after 80km transmission. Solid lines are the results of the proposed method and dashed lines are the results of the sweeping method. (b) BERs with different alphas applied under CSPR = 6 dB.

We mainly focus on the situation where the BER is about 3.8×10^{-3}. Solid lines are the results of our proposed data-aided method and the dashed lines are the results of traditional sweeping method. The BER is about 3.8×10^{-3} when the optical power is around -11 dBm and CSPR is 10 dB. With a constant overall power, higher CSPR means lower payload signal power. When optical power is low, a lower CSPR is preferred because it provides more useful power. While with a higher optical power, a higher CSPR performs better as it benefits the outer ring of 16-QAM. Fig. 6(b) shows the trend of BER with coefficient α. The α has a similar tendency to simulation results, but deviates more from 1, due to the more complicated environment of experiments compared to simulations. A lower received optical power prefers a larger α, because higher DC value helps to suppress the phase jumps [6]. The estimation error of α based on the data-aided method is within a tolerable range of about 10% even when the received optical power is insufficient. With comparatively sufficient optical power, the deviation of α becomes smaller and it is about 3% when the received optical power is -9 dBm. Fig. 6(b) also shows that by correcting the estimation with optimal α, the system performance is further improved when the optical power is insufficient. However, with sufficient signal power, the estimation by our proposed method is accurate enough.

We also test our proposed data-aided method with various CSPRs after 80 km transmission. The signal after PMOC is first amplified by an EDFA to 9 dBm, then goes through SMF and is detected by an AC-coupled PD. The received optical power is about -9 dBm. We compare the BER performance to the sweeping method by sweeping α as we did in back-to-back situations. The results after transmission are exhibited in Fig. 7. In Fig. 7(a), the solid line representing the results of data-aided method is close to the dashed line that represents the results of the sweeping method. Such Ber performance is accordant to that in the back-to-back scenario, only with a reasonable degradation. The α has a deviation of about 5% compared to the optimal value from the sweeping method as Fig. 7(b) shows. Our proposed data-aided method shows its credibility and stability after fiber transmission as it does in back-to-back transmissions.

IV. CONCLUSION

In conclusion, we propose a simple method to estimate the DC component isolated by an AC-coupled photodetector. Using data-aided sequences with constant moduli, we succeed in accurately recovering the DC component after simple mathematical calculation. Our method requires no physical structures and all work can be done in the digital domain. Compared to the existing method, our method shows better accuracy and stability. We carry out simulations and transmission experiments to investigate our method. In order to validate the reliability of our method, we conduct an experiment of transmitting a 3 GBaud 16-QAM SSB signal both in the back-to-back and 80 km SMF transmission scenarios. The BER is about 3.8×10^{-3} when the optical power is around -11 dBm and CSPR is 10 dB. Compared to the estimation of the traditional sweeping method, our proposed method shows a similar performance and higher efficiency. The deviation of α is about 3% when the optical power is sufficient. Even with insufficient received optical power, the difference represented by α is floating within a range of 10%. Compared to other DC estimation methods, our data-aided method is simple and flexible with better stability. It only costs a negligible length of the data-aided sequence, if there is no data-aided sequence that already exists. Besides, the data-aided sequences are not fixed and can also be designed to any form as long as the power and phase satisfy our principles. That means the sequences used in further estimations and equalizations can also be used for our method easily. Therefore, we believe our method is practical for applications of the KK-receiver

REFERENCES

[1] M. Filer, J. Gaudette, Y. Yin, D. Billor, Z. Bakhtiari, and J. L. Cox, "Low-margin optical networking at cloud scale," *IEEE/OSA J. Opt. Commun. Netw.*, vol. 11, no. 10, pp. C94–C108, Oct. 2019.

[2] A. Mecozzi, C. Antonelli, and M. Shtaif, "Kramers-Kronig coherent receiver," *Optica*, vol. 3, no. 11, pp. 1220–1227, Nov. 2016.

[3] Z. Li *et al.*, "SSBI mitigation and the Kramers–Kronig scheme in single-sideband direct-detection transmission with receiver-based electronic dispersion compensation," *J. Lightw. Technol.*, vol. 35, no. 10, pp. 1887–1893, May. 2017.

[4] A. Mecozzi, C. Antonelli, and M. Shtaif, "Kramers-Kronig receivers," *Adv. Opt. Photon.*, vol. 11, no. 3, pp. 480–517, Sep. 2019.

[5] S. An, Q. Zhu, J. Li, and Y. Su, "Modified KK receiver with accurate field reconstruction at low CSPR condition," in *Proc. Opt. Fiber Commun. Conf. Exhib.*, 2019, pp. 1–3.

[6] T. Bo and H. Kim, "DC component recovery in kramers-kronig receiver utilizing AC-coupled photo-detector," *J. Lightw. Technol.*, vol. 38, no. 16, pp. 4307–4314, Aug. 2020.

[7] T. Bo and H. Kim, "Kramers-Kronig receiver without digital upsampling," in *Proc. Opt. Fiber Commun. Conf. Expo.*, 2018, pp. 1–3.

[8] T. Bo and H. Kim, "Toward practical Kramers-Kronig receiver: Resampling, performance, and implementation," *J. Lightw. Technol.*, vol. 37, no. 2, pp. 461–469, Jan. 2019.

[9] X. Li *et al.*, "Asymmetric direct detection of orthogonal offset carriers assisted polarization multiplexed single-sideband signals," *Opt. Exp.*, vol. 28, no. 3, pp. 3226–3236, Feb. 2020.

[10] Y. Zhu, M. Jiang, and F. Zhang, "Direct detection of polarization multiplexed single sideband signals with orthogonal offset carriers," *Opt. Exp.*, vol. 26, no. 12, pp. 15887–15898, Jun. 2018.

[11] Y. Zhou, J. Yu, Y. Wei, J. Shi, and N. Chi, "Four-channel WDM 640 Gb/s 256 QAM transmission utilizing Kramers-Kronig receiver," *J. Lightw. Technol.*, vol. 37, no. 21, pp. 5466–5473, Nov. 2019.

[12] S. T. Le, K. Schuh, R. Dischler, F. Buchali, L. Schmalen, and H. Buelow, "Beyond 400 Gb/s direct detection over 80 km for data center interconnect applications," *J. Lightw. Technol.*, vol. 38, no. 2, pp. 538–545, Jan. 2020.

[13] X. Chen *et al.*, "Kramers–Kronig receivers for 100-km datacenter interconnects," *J. Lightw. Technol.*, vol. 36, no. 1, pp. 79–89, Jan. 2018.

[14] Z. Li *et al.*, "Spectrally efficient 168 Gb/s/λ WDM 64-QAM single-sideband Nyquist-subcarrier modulation with Kramers–Kronig direct-detection receivers," *J. Lightw. Technol.*, vol. 36, no. 6, pp. 1340–1346, Mar. 2018.

[15] Z. Tu, A. Wen, G. Yu, X. Li, and H. Zhuo, "A wideband photonic RF receiver with lower IF frequency enabled by Kramers–Kronig detection," *J. Lightw. Technol.*, vol. 37, no. 20, pp. 5309–5316, Oct. 2019.

[16] J. Blumenstein and M. Bobula, "Coarse time synchronization utilizing symmetric properties of Zadoff–Chu sequences," *IEEE Commun. Lett.*, vol. 22, no. 5, pp. 1006–1009, May. 2018.

[17] A. V. Tran *et al.*, "8×40-Gb/s optical coherent pol-mux single carrier system with frequency domain equalization and training sequences," *IEEE Photon. Technol. Lett.*, vol. 24, no. 11, pp. 885–887, Jun. 2012.

[18] X. Zhou, "Digital signal processing for coherent multi-level modulation formats," *Chin. Opt. Lett.*, vol. 8, no. 9, pp. 863–870, Sep. 2010.

[19] X. Zhou *et al.*, "PDM-nyquist-32QAM for 450-Gb/s per-channel WDM transmission on the 50 GHz ITU-T grid," *J. Lightw. Technol.*, vol. 30, no. 4, pp. 553–559, Feb. 2012.